

Reaction of Tungsten η^1 -Acetylide Complexes $[(\eta^5\text{-C}_5\text{H}_5)(\text{NO})(\text{CO})\text{W}-\text{C}\equiv\text{C}-\text{R}]\text{Li}$ with Iminium Ions

Junes Ipaktschi,^{*,†} Javad Mohsseni-Ala,[†] Ansgar Dülmer,[†]
 Christoph Loschen,[‡] and Gernot Frenking[‡]

*Institute of Organic Chemistry, Justus-Liebig University, Heinrich-Buff-Ring 58,
 D-35392 Giessen, Germany, and Fachbereich Chemie, Philipps-Universität Marburg,
 Hans-Meerwein-Strasse, D-35043 Marburg, Germany*

Received November 15, 2004

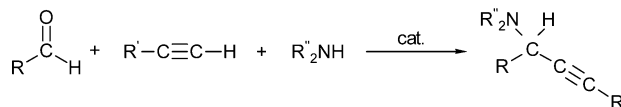
The reaction of alkynyltungsten complexes $[(\text{CO})(\text{NO})(\text{Cp})\text{W}-\text{C}\equiv\text{C}-\text{R}]\text{Li}$ ($\text{R} = \text{H}, \text{C}_6\text{H}_5, \text{C}(\text{CH}_3)_3$) with differently substituted iminium ions is investigated. Due to the relative high acidity of the hydrogen atoms on the β -carbon atom of the η^1 -vinylidene complex $[(\text{CO})(\text{NO})(\text{Cp})\text{W}=\text{C}=\text{CH}_2]$ (**1**), the parent η^1 -acetylide complex $[(\text{CO})(\text{NO})(\text{Cp})\text{W}-\text{C}\equiv\text{C}-\text{H}]^-$ is generated in situ simultaneously with the iminium ion by the reaction of η^1 -vinylidene complex **1** with an enamine. The reaction of **1** with enamines **2a–e** leads to vinylcarbene complexes **3a–e** in good yield. The first step of this transformation is a Mannich reaction on the β -carbon atom of alkynyltungsten complexes, generating the expected β -amino-alkylated η^1 -vinylidene complexes **6**. This intermediate reacts further to **3a–e** by migration of the hydrogen atom adjacent to the nitrogen atom to the α -carbon atom of the η^1 -vinylidene moiety. The appearance of a η^1 -vinylidene complex as an intermediate is supported by NMR experiments, and the postulated retro-imino-ene reaction is confirmed by the reaction of deuterated η^1 -vinylidene complex **1-D** with enamine **2b** to the vinylcarbene complex **8**. The scope of the reaction is demonstrated by the reaction of alkynyltungsten complexes **9**, **16**, and **17** with a series of differently substituted iminium ions to the corresponding vinylcarbene complexes. Activation parameters for the retro-imino-ene reaction of η^1 -vinylidene complex **6a** to vinylcarbene **3a** in THF-*d*₈ were determined using ¹H NMR spectroscopy. On the basis of this experiment ΔH^\ddagger , ΔS^\ddagger , and ΔG^\ddagger (at -1°C) were found to be 20.5 ± 1.4 kcal/mol, -1.4 ± 0.6 cal/mol, and 20.9 ± 1.4 kcal/mol, respectively. The profile of the postulated retro-imino-ene reaction is calculated on the model compound $[(\text{CO})(\text{NO})(\text{Cp})\text{W}=\text{C}=\text{CH}-\text{CH}_2-\text{NH}-\text{CH}_3]$ (**6M**), yielding $[(\text{CO})(\text{NO})(\text{Cp})\text{W}=\text{CH}-\text{CH}=\text{CH}_2]$ using density functional theory at the B3LYP level. The calculation shows the process is more likely a single-step reaction where the hydrogen migration and carbon–nitrogen bond breaking are two consecutive reactions without formation of a true intermediate. Single-crystal X-ray diffraction data of **3a** and **4** are reported.

Introduction

Much attention has been devoted to the intramolecular as well as intermolecular reaction of mono- and disubstituted alkynes with iminium ions.¹ Reaction of terminal alkynes with iminium ions were investigated already by Mannich and are a well-established method for the synthesis of propargylamines (Scheme 1).² A highly efficient modification of this reaction, a three-component coupling of aldehydes, alkynes, and amines catalyzed by copper or gold salts, was recently described by different research groups.³

Contrary to the terminal alkynes, dialkyl-substituted derivatives are not sufficiently nucleophilic to react with

Scheme 1



simple iminium ions, and usually activation of iminium ion for example through acylation is necessary.¹ Alternatively the presence of a reactive internal or assistance of an external nucleophile such as iodide ion helps to initiate the reaction.⁴ *N*-Acyliminium ion is an example of an activated iminium ion, and its reaction with dialkyl-substituted alkynes is used frequently for the

* To whom correspondence should be addressed. E-mail: junes.ipaktschi@org.chemie.uni-giessen.de. Fax: (+49) 641-99 34 309.

[†] Justus-Liebig University.

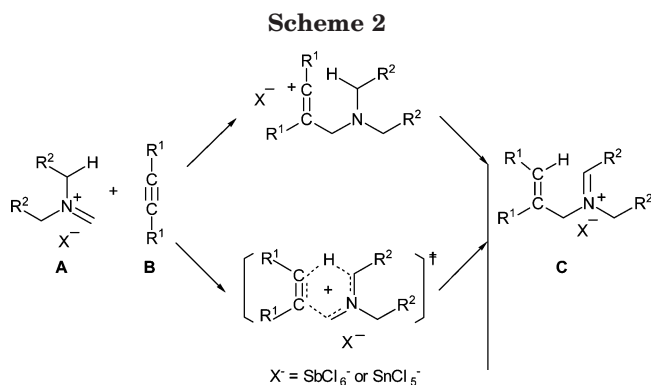
[‡] Philipps-Universität Marburg.

(1) For comprehensive review see: Maryanoff, B. E., Zhang, H., Cohen, J. H., Turchi, I. J., Maryanoff, C. A. *Chem. Rev.* **2004**, *104*, 1431.

(2) (a) Mannich, C.; Chang, F. T. *Ber. Dtsch. Chem. Chem. Ges.* **1933**, *66*, 418. (b) Coffman, D. D. *J. Am. Chem. Soc.* **1935**, *57*, 1978. (c) Jones, E. R. H.; Marszak, I.; Bader, H. *J. Chem. Soc.* **1947**, 1578.

(3) (a) Chunmei, W.; Chao-Jun, L. *J. Am. Chem. Soc.* **2003**, *125*, 9584. (b) Koradin, C.; Polborn, K. Knochel, P. *Angew. Chem.* **2002**, *114*, 2651; *Angew. Chem., Int. Ed.* **2002**, *41*, 2535. (c) Tramontini, M.; Angiolini, L. *Tetrahedron* **1990**, *46*, 1791. (d) Tramontini, M. *Synthesis* **1973**, 703.

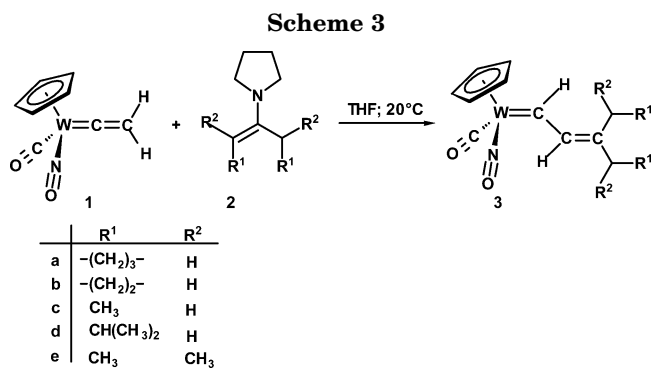
(4) (a) Franklin, A. S.; Overman, L. E. *Chem. Rev.* **1996**, *96*, 505. (b) Overman, L. E.; Rodriguez-Campos, I. M. *Synlett* **1992**, 995. (c) Arnold, H.; Overman, L. E.; Sharp, J.; Witschel, M. C. *Org. Synth.* **1992**, *70*, 11. (d) Overman, L. E.; Sharp, M. J. *J. Am. Chem. Soc.* **1988**, *110*, 613.



syntheses of a broad variety of heterocyclic compounds.^{1,5} It is generally discussed that in the first step of the reaction a vinyl cation is formed as an intermediate.¹ In the course of further reaction, this cation is captured by solvent or an available anion^{5b,d} or through an intramolecular reaction with a nucleophile moiety of the same molecule. An example is the Pictet–Spengler approach for the synthesis of heterocyclic compounds by using activated alkynes.⁶ There are also numerous examples of Mannich reactions in which propargylsilanes are effective nucleophiles.^{1,7} The transformation is usually accompanied by elimination of the silicon moiety from the incipient vinyl cation to form an allene as the final product.⁸

An interesting example observed recently is the reaction of internal alkynes with iminium ions in the absence of internal as well as external nucleophiles in solvents with low nucleophilicity. When the iminium hexachloroantimonates or pentachlorostannate **A** is combined with alkyne **B** in dichloromethane, *N*-alkyl-*N*-allylalkylidene ammonium salt **C** is formed in high yield.⁹ This reaction has similarity to an ene reaction with inverse electron demand and is conceivable as either a multistep or concerted process described in Scheme 2. The key step of this transformation is a hydride shift, quasi as an internal nucleophile, from the α -carbon atom of iminium ion to the incipient vinyl cation.

Alkynyltungsten complexes $[(\text{CO})(\text{NO})(\text{Cp})\text{W}-\text{C}\equiv\text{C}-\text{R}]\text{Li}$ are a versatile electron-rich acetylene derivative and has an ample chemistry. Reaction of these anions with “hard” electrophiles led to η^1 -vinylidene complexes.^{10b,c,e} “Soft” electrophiles such as allyliodide, 1,2-iodoethane, or ethyliodoacetate attack predominantly at the tungsten atom,^{10a,d} and the addition of strong nucleophiles such as *n*-C₄H₉-Li occurs at the carbon



atom of the carbonyl group.^{10a} To shed light on the mechanism of the reaction of iminium ions with internal alkynes and to trap a possible intermediate, we investigated the Mannich reaction of anionic η^1 -acetylene complexes $[(\text{CO})(\text{NO})(\text{Cp})\text{W}-\text{C}\equiv\text{C}-\text{R}]^-$ (R = H, *tert*-butyl, Ph) with different iminium ions. Due to the relative high acidity of the hydrogen atoms on the β -carbon atom of the η^1 -vinylidene complexes,^{10c} the parent η^1 -acetylide complex $[(\text{CO})(\text{NO})(\text{Cp})\text{W}-\text{C}\equiv\text{C}-\text{H}]^-$ is generated more conveniently in situ simultaneously with the desired iminium ion by the reaction of η^1 -vinylidene complex **1** with an enamine (Scheme 3). Alternatively the substituted η^1 -acetylene complexes $[(\text{CO})(\text{NO})(\text{Cp})\text{W}-\text{C}\equiv\text{C}-\text{R}]\text{Li}$ (R = *tert*-butyl, Ph) as well as the parent anion are generated by the reaction of the corresponding η^1 -vinylidene complexes with *n*-C₄H₉-Li.

Results and Discussion

Reaction of η^1 -Vinylidene Complex 1 with Enamines 2a–e. When a solution of readily available η^1 -vinylidene complex **1** in THF is treated at room temperature with 1 equiv of enamines **2a–d**, the color of the solutions changed immediately from red to deep red. After 1 h, the vinylcarbene complexes **3a–d** (Scheme 3) were isolated in 50–60% yield as a mixture of two stereoisomers in a ratio of 1:7 up to 1:30 by appropriate workup and chromatography on silica. Either this stereoisomerism is based on the relative orientation of NO and CO ligands toward the 2-propenylidene unit, or the orientation of propenylidene ligand toward the cyclopentadienyl ring, “*Z*” or “*E*”, is responsible for the ratio of isomers.

The sterically hindered enamine **2e** undergoes a much slower reaction with the η^1 -vinylidene complex **1**. Treatment of a solution of complex **1** in THF with 3 equiv of enamine **2e** at room temperature for 12 h resulted in formation of vinylcarbene complex **3e** as a 1:15 mixture of two rotamers in 37% yield, which was isolated by column chromatography. In addition to **3e**, this reaction afforded the aminocarbene complex **4** in 12% yield as orange crystals (Scheme 4). Complexes **3a–e** are soluble in organic solvents and could be stored without decomposition at -20°C under an argon atmosphere for

(5) (a) Huang, H.-L.; Sung, W.-H.; Liu, R.-Shung, *J. Org. Chem.* **2001**, *66*, 6193. (b) Caderas, C.; Lett, R.; Overman, L. E.; Rabinowitz, M. H.; Robinson, L. A.; Sharp, M. J. *J. Am. Chem. Soc.* **1996**, *118*, 9073. (c) Fisher, M. J.; Overman, L. E. *J. Org. Chem.* **1990**, *55*, 1447. (d) Lin, N.; Overman, L. E.; Rabinowitz, M. H.; Robinson, L. A.; Sharp, M. J.; Zablocki, J. *J. Am. Chem. Soc.* **1996**, *118*, 9062.

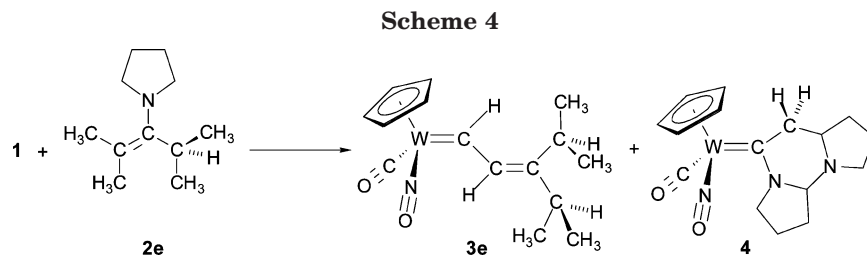
(6) Vercauteren, J.; Lavaud, C.; Lévy, J.; Massiot, G. *J. Org. Chem.* **1984**, *49*, 2278.

(7) (a) Consonni, A.; Danieli, B.; Lesma, G.; Passerella, D.; Piacenti, P.; Silvani, A. *Eur. J. Org. Chem.* **2001**, 1377. (b) Karstens, W. F. J.; Moolenaar, M. J.; Rutjes, F. P. J. T.; Grabowska, U.; Speckamp, W. N.; Hiemstra, H. *Tetrahedron Lett.* **1999**, *40*, 8629. (c) Luker, T.; Koot, W.-J.; Hiemstra, H.; Speckamp, W. N. *J. Org. Chem.* **1998**, *63*, 220.

(8) Reich, H. J.; Yelm, K. E.; Reich, I. L. *J. Org. Chem.* **1984**, *49*, 3438.

(9) (a) Rehn, S.; Ofial, A. R.; Mayr, H. *Synthesis* **2003**, 1790. (b) Ofial, A. R.; Mayr, H. *Angew. Chem.* **1997**, *109*, 145; *Angew. Chem., Int. Ed. Engl.* **1997**, *36*, 143.

(10) (a) Ipaktschi, J.; Reimann, K.; Serafin, M.; Dülmer, A. *J. Organomet. Chem.* **2003**, *670*, 66. (b) Ipaktschi, J.; Munz, F. *Organometallics* **2002**, *21*, 977. (c) Ipaktschi, J.; Mohsseni-Ala, J.; Uhlig, S. *Eur. J. Inorg. Chem.* **2003**, 4313. (d) Ipaktschi, J.; Mirzaei, F.; Demuth-Eberle, G. J.; Beck, J.; Serafin, M. *Organometallics* **1997**, *16*, 3965. (e) Ipaktschi, J.; Müller, B.; Glaum, R. *Organometallics* **1994**, *13*, 1044.

**Table 1. Selected NMR Spectral Data for Vinylcarbene Complexes 3a–e, 8, 19–21, and 23^a**

complex	stereoisomer ratio	δ H $_{\alpha}$ ppm	δ H $_{\beta}$ ppm	J (H $_{\alpha}$ –H $_{\beta}$) Hz	δ C $_{\alpha}$ ppm
3a	1:8	15.03; 14.20	8.04; 7.21	14.7; 13.2	274.2
3b	1:7	14.70; 13.78	8.18; 7.35	14.8; 13.2	276.3
3c	1:7	14.93; 14.10	7.98; 7.14	14.7; 13.1	275.2
3d	1:30	14.95; 14.07	8.04; 7.26	12.0; 13.1	275.5
3e	1:15	15.12; 14.29	8.11; 7.28	12.0; 13.2	274.5
8	1:10	14.65; 13.82			276.2
19	1:23	14.51; 13.72	8.03; 7.25	12.3; 12.2	283.5
20	1:8	15.47; 14.38			273.7; 273.4
21	1:15	14.91; 14.07	8.08; 7.26	12.0; 12.0	274.9
23	1:10	14.60; 13.72	8.01; 7.20	12.3; 12.3	283.1

^a All spectra were acquired in CDCl₃.

several months. However, aminocarbene complex **4** is unstable under similar conditions and decomposes over time.

The unequivocal characterization of complexes **3a–e** and **4** was achieved by means of elemental analysis and from standard spectroscopic techniques. The structures of products are further confirmed by the result of single-crystal structure analysis of **3a** and **4**. The reaction of η^1 -vinylidene complex **1** with enamines **3a–e** is accompanied by a shift of the carbonyl absorptions of the Cp(CO)(NO)W fragment toward lower wavenumbers (from 2000 to 1965–1989 cm⁻¹). Additionally the IR spectra of **3a–e** show two strong bands in the 1561–1596 cm⁻¹ region for the nitrosyl ligand. The ¹H and ¹³C NMR spectra reveal the presence of the 2-propenylidene groups. The most relevant data arise from the typical low-field carbene carbon (C $_{\alpha}$) resonances at δ 274.2–276.3 ppm.¹¹ The more upfield resonances are assigned to the remaining two carbon atoms of the 2-propenylidene chain (e.g., δ 141.0–154.9 ppm for C $_{\beta}$ and C $_{\gamma}$). The ¹H NMR spectra also show downfield resonances at δ 13.58–15.12 ppm, which are characteristic of the W=CH proton.¹¹ In particular, the ¹H NMR spectra show coupling constants characteristic for an *s-trans* arrangement of the 2-propenylidene group in complexes **3a–e** (large proton coupling constant between H $_{\alpha}$ and H $_{\beta}$). The most informative data of ¹H and ¹³C NMR spectra for **3a–e** are listed in Table 1.

Also elemental analysis and spectroscopic data of **4** are in accord with the proposed structure. The IR spectra of **4** exhibit a strong carbonyl band at 1899 cm⁻¹ and a strong signal for the nitrosyl group at 1560 cm⁻¹. These stretching frequencies are comparable to the CO and NO absorptions in similar aminocarbene complexes.¹² In agreement with the structure, the ¹³C NMR

spectrum of complex **4** shows a signal at δ 251.0 ppm, in the characteristic range for the carbene carbon of the aminocarbene complexes.¹²

Mechanistic Considerations. As a working hypothesis for the formation of **3a–e** and **4** by the reaction of enamines **2a–e** with the η^1 -vinylidene complex **1** we suppose that the reaction starts with the acid/base process (a) leading to an aggregate of tungsten η^1 -acetylide complex–iminium ion pair **5** (Scheme 5). Although the pK $_{\text{a}}$ value of the η^1 -vinylidene tungsten complexes are not determined yet, we assume high acidity for the proton on the β -carbon atom of these complexes. Recently we have shown that η^1 -vinylidene tungsten complexes containing a hydrogen atom on the β -carbon atom undergo deprotonation–protonation reactions very easily, which was determined by a H/D exchange experiment in THF/D₂O.^{10c} Subsequently in a Mannich-type reaction the β -carbon atom of anionic tungsten η^1 -acetylide complex is amino alkylated by the iminium ion to give rise to the η^1 -vinylidene complex **6** as a reactive intermediate (step b).^{5a}

In final and crucial step (c), very similar to the one discussed in Scheme 2, η^1 -vinylidene complex **6** undergoes a retro-imino-ene reaction¹³ by transferring a hydrogen atom from the α -carbon atom of the pyrrolidine ring to the central carbon atom of the η^1 -vinylidene moiety and fragment to the vinylcarbene complexes **3a–e** and 1-pyrroline (**7**). It is surprising that this retro-imino-ene step occurs readily below room temperature. Although retro-ene type fragmentations have been extensively studied, very few examples of retro-imino-ene reactions are reported in the literature.¹³ In general these reactions are carried out at high temperature and low pressure. A typical example is the fragmentation of propargylic amines, which occurs at 650–680 °C and 10⁻³–10⁻⁴ Torr to give allene and the corresponding imino derivative (Scheme 6).¹⁴

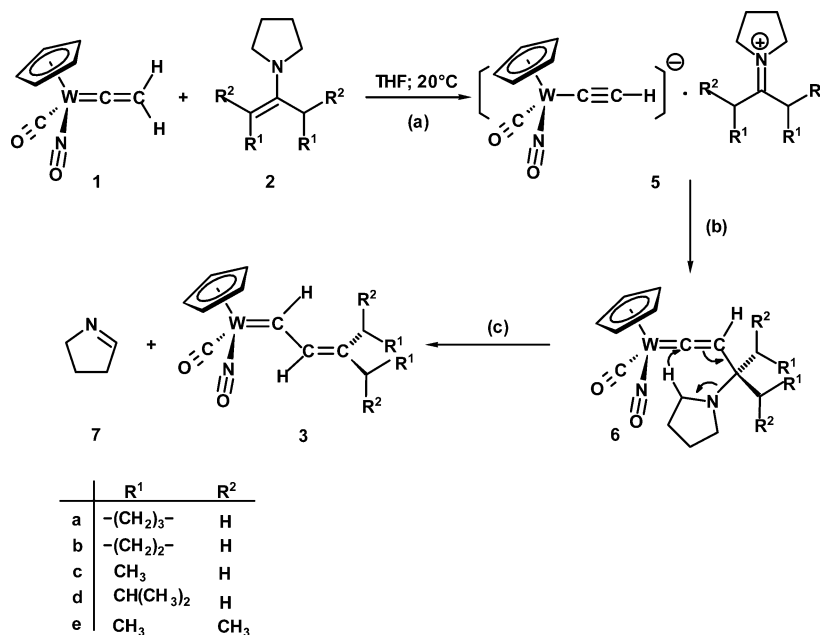
(11) (a) Yi, C. S.; Geoffroy, G. L. *J. Am. Chem. Soc.* **1993**, *115*, 3806. (b) Johanes, L. K.; Grubbs, R. H.; Ziller, J. W. *J. Am. Chem. Soc.* **1993**, *115*, 8130. (c) Schrock, R. R. In *Reaction of Coordinated Ligands*; Brateman, P. S., Ed.; Plenum: New York, 1986; Vol. 1, pp 221–283.

(12) (a) Ipaktschi, J.; Mohseni-Ala, J.; Dülmer, A.; Steffens, S.; Wittenburg, C.; Heck, J. *Organometallics* **2004**, *23*, 4902. (b) Ipaktschi, J.; Uhlig, S.; Dülmer, A. *Organometallics* **2001**, *20*, 8440.

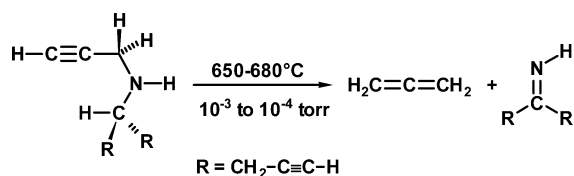
(13) (a) Borzilleri, R. M.; Weinreb, S. M. *Synthesis* **1995**, 347. (b) Viola, A.; Collins, J. J.; Filipp, N. *Tetrahedron* **1981**, *37*, 3765.

(14) Viola, A.; Collins, J. J.; Filipp, N.; Locke, J. S. *J. Org. Chem.* **1993**, *58*, 5067.

Scheme 5



Scheme 6



By considering the electronic features of the ligands on the tungsten atom of η^1 -vinylidene complex **6**, the observed low activation energy for the retro-imino-ene reaction is understandable.

A conceivable alternative to the above reaction mechanism is given in Scheme 7. In this option a η^1 -vinylidene complex is not formed as an intermediate. The transformation of tungsten η^1 -acetylide complex to the observed products starts with an ene reaction with the iminium ion generating the iminium ion **D**, which by elimination of 1-pyrroline produces the observed vinylcarbene complexes.

Unfortunately we could not isolate the 1-pyrroline, the expected second product of the reaction from our reaction mixture. It is known that 1-pyrroline is thermally in equilibrium with 1,3,5-triazine and is easily removed during the evaporation of solvent under vacuum.¹⁵

To distinguish between the two alternative reaction mechanisms and to support the reaction path presented in Scheme 5, we investigated first the reaction of deuterated η^1 -vinylidene complex **1-D** with enamine **2b** and further attempted to identify the η^1 -vinylidene complex intermediate postulated in the first reaction mechanism by the reaction of η^1 -acetylide complex **9** with iminium ions **10** and **11**.

In accordance with the mechanistic paths proposed in Schemes 5 and 7, reaction of η^1 -vinylidene complex **1-D** with enamine **2b** led to the vinylcarbene complex

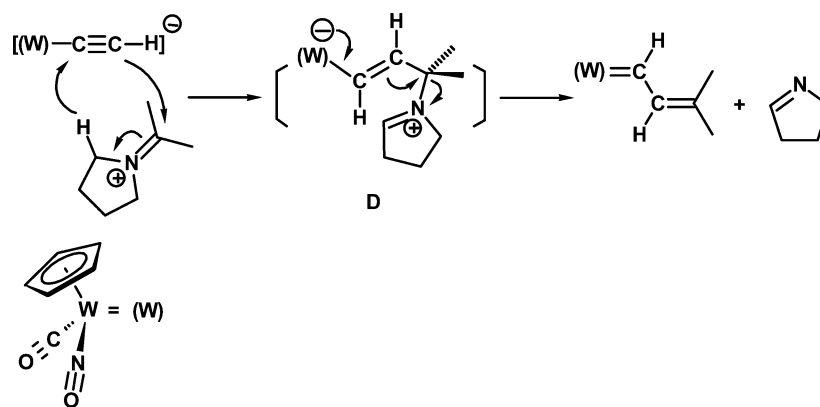
8 (Scheme 8). The structure of **8** was clearly determined by CHN analysis and spectroscopic methods. The most informative features from the ¹H NMR spectra are two singlet signals for H_α at δ 14.65 and 13.82 ppm (ratio 1:10; two stereoisomer) and the absence of signals for H_β. The integral of the signal at δ 2.12–2.03 ppm (m, 3H) shows the incorporation of a deuterium atom at the α-carbon atom of the cyclopentylidene ring of complex **8**. The signal at δ 1.76–1.64 ppm (m, 4H) remains unchanged in comparison to the corresponding signal of **3b**. This result shows that one deuterium atom of η^1 -vinylidene complex **1-D** is transferred to the β-position of enamine and the hydrogen atom on the α-carbon atom of **8** originates from the α' position of enamine **2b**.

Characterization of η^1 -vinylidene derivatives **6**, postulated in Scheme 5 as an intermediate, was more conveniently achieved by monitoring the reaction of η^1 -acetylide complex **9** with iminium perchlorate **10** using IR and UV/vis spectroscopy as well as the reaction of η^1 -acetylide complex **9** with the iminium perchlorate **11** by NMR spectroscopic techniques. Alternatively to the in situ generation of the aggregate of tungsten η^1 -acetylide complex–iminium ion pair **5** the η^1 -acetylide complex **9** was prepared as an emerald green solution in THF by deprotonation of the corresponding η^1 -vinylidene complex **1** with *n*-C₄H₉Li at –78 °C and subjected to Mannich reaction with presynthesized iminium perchlorate **10**. The IR spectrum of **9** shows in THF at –64 °C a strong carbonyl band at 1864 cm^{–1} and a broad signal for the nitrosyl group at 1460 cm^{–1}. After addition of 1 equiv of iminium perchlorate **10** at –78 °C to the green solution of **9** in THF under an argon atmosphere, in the IR spectra the absorptions for the carbonyl and nitrosyl groups disappear during 2 h. New strong signals at 1986 cm^{–1} and 1643 and 1614 cm^{–1} are in the region of CO and NO signals of similar η^1 -vinylidene complexes in the IR spectrum^{10c,16} and also

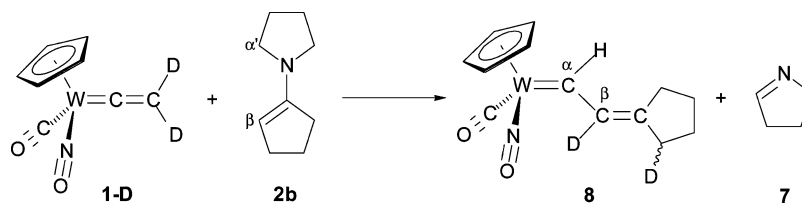
(15) (a) Cantrell, G. K.; Geib, S. J.; Meyer, T. J. *Organometallics* **2000**, *19*, 3562. (b) Wiberg, K. B.; Nakaji, D. Y.; Morgan, K. M. *J. Am. Chem. Soc.* **1993**, *115*, 3527.

(16) (a) Ipaktschi, J.; Klotzbach, T.; Dülmer, A. *Organometallics* **2000**, *19*, 5281. (b) Ipaktschi, J.; Demuth-Eberle, G. J.; Mirzaei, F.; Müller, B. G.; Beck, J.; Serafin, M. *Organometallics* **1995**, *14*, 3335.

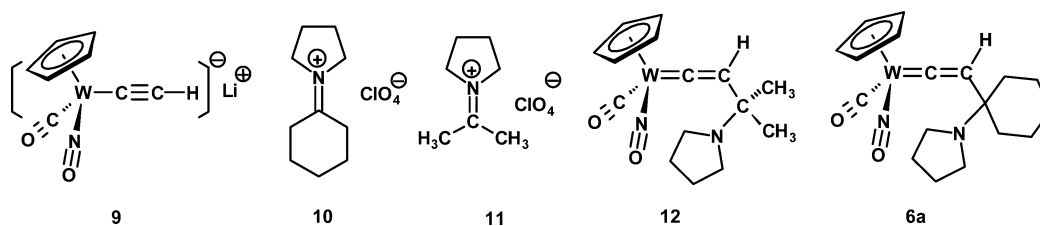
Scheme 7



Scheme 8



Scheme 9



which are assigned to the η^1 -vinylidene complex **6a** (1986 cm^{-1} CO, and 1643 and 1614 cm^{-1} NO).

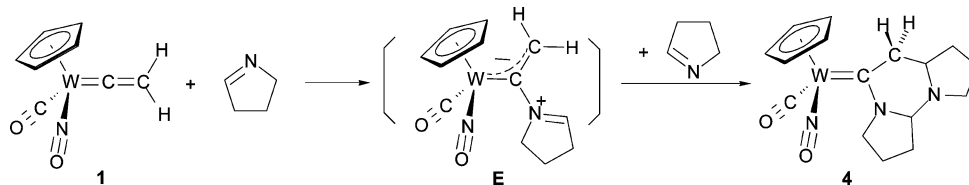
Through warming the above reaction solution to room temperature the carbonyl and nitrosyl absorptions of **6a** disappear and the signals for carbonyl and nitrosyl groups of vinylcarbene complex **3a** appear at 1973 cm^{-1} (carbonyl group) and at 1606 and 1575 cm^{-1} for the nitrosyl ligand. Likewise to the above monitoring of the reaction by infrared spectroscopy, the addition of iminium perchlorate **10** to η^1 -acetylide complex **9** was monitored by UV/vis spectroscopy. The η^1 -acetylide complex **9** shows at -78 °C in THF an absorption maximum at 606 nm ($\log \epsilon = 1.57$). After addition of 1 equiv of iminium perchlorate **10** to the green solution of complex **9** under argon atmosphere, the color changed to red, the UV absorption of complex **9** vanished, and the UV/vis spectra show two new absorption maxima at 454 nm ($\log \epsilon = 2.13$) and 309 nm ($\log \epsilon = 3.81$) together with a shoulder at 363 nm similar to the UV/vis spectrum of tungsten η^1 -vinylidene complexes **1** ($\lambda_{\text{max}} = 440$ nm ($\log \epsilon = 2.43$) and 267 nm ($\log \epsilon = 4.07$) and a shoulder at 357 nm) and **15** ($\lambda_{\text{max}} = 460$ nm ($\log \epsilon = 2.35$) and 272 nm ($\log \epsilon = 4.16$) and a shoulder at 360 nm). Three isobestic points at 409, 420, and 523 nm indicate that complex **9** is completely transformed into this reactive intermediate, which is assigned to η^1 -vinylidene complex **6a**. Warming the reaction mixture to room temperature led to the formation of a strong UV absorption at 374 nm ($\log \epsilon = 4.11$) and a shoulder at 340 nm), which is assigned to the vinylcarbene complex **3a** through comparison with the UV/vis spectra

of an authentic sample. The observation of an isobestic point at 325 nm demonstrates the complete conversion of intermediate **6a** to **3a**.

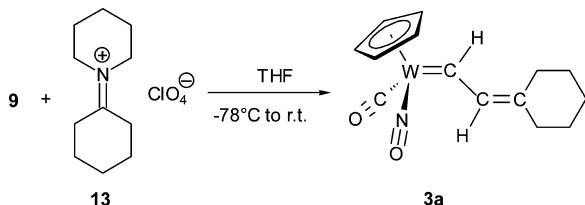
To confirm further the appearance of a η^1 -vinylidene complex as intermediate, the reaction was monitored also by NMR spectroscopy. For this purpose 0.15 mmol of complex **9** in 0.8 mL of THF- d_8 was treated under argon atmosphere in a NMR tube at -78 °C with 0.15 mmol of iminium perchlorate **11**. The resulting reaction mixture showed in the ^1H NMR spectra two signals at δ 6.05 and 6.03 ppm (ratio 1:1) for Cp and two signals at δ 5.68 and 5.67 ppm (ratio 1:1) for C_βH , and analogously in ^1H NMR spectra to similar η^1 -vinylidene complexes.^{16b} The most relevant data arise from the ^{13}C NMR spectra, which show the typical low-field C_α resonances of η^1 -vinylidene complexes at δ 336.01 ppm with $^1J(^{183}\text{W}-^{13}\text{C}) = 185.9$ Hz and δ 334.66 ppm with $^1J(^{183}\text{W}-^{13}\text{C}) = 181.7$ Hz.^{16b} Annealing of the probe to room temperature led to the formation of new signals at δ 14.87 and 14.12 ppm (ratio 1:7), δ 8.01 and 7.22 ppm (ratio 7:1), and δ 5.97 and 5.94 ppm (ratio 7:1), which are assigned to the vinylcarbene complex **21** through comparison with the ^1H NMR spectrum of an authentic sample.

The tricyclic aminocarbene complex **4** contain two units of 1-pyrroline. We suppose that for the formation of this complex the low reactivity of the enamine **2e** toward **1** is responsible. The highly reactive 1-pyrroline produced by the reaction of **1** with **2e** attacks the α -carbon atom of unreacted η^1 -vinylidene complex **1** producing the betaine **E**, which is then trapped by a

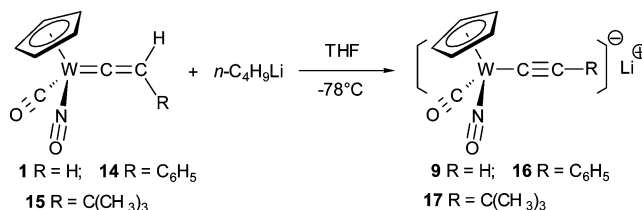
Scheme 10



Scheme 11



Scheme 12



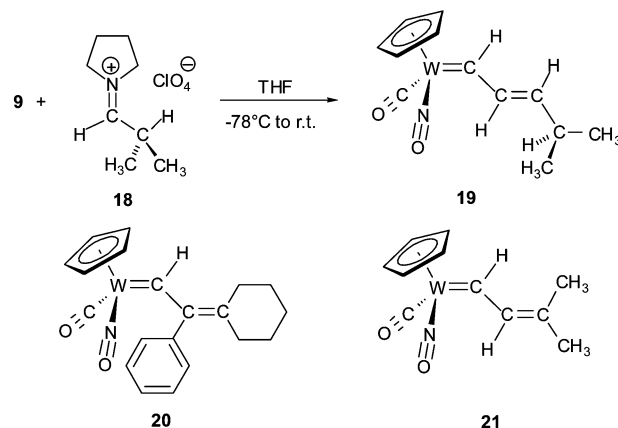
second molecule of 1-pyrrolidine to the tricyclic compound **4** (Scheme 10).

Reaction of η^1 -Acetylide Complexes with Iminium Ions. To test the scope of the retro-imino-ene reaction, we next examined iminium ions containing amine components other than pyrrolidine. The reaction of **9** with the iminium perchlorate **13** shows that the hydrogen atom is transferred from the α -carbon atom of the piperidine ring as easily as from the α -carbon atom of the pyrrolidine ring. Analogous to the iminium ion **10** the addition of 1 equiv of iminium perchlorate **13** to a solution of η^1 -acetylide complex **9** in THF at -78°C and warming to room temperature led to complex **3a** with 52% yield (Scheme 11).

Likewise, the addition of 1 equiv of iminium perchlorates **10**, **11**, and **18** to the η^1 -acetylide complex **9** and iminium ion **10** to η^1 -acetylide complex **16** gave rise after usual workup and chromatography to the vinylcarbene complexes **3a**, **21**, **19**, and **20** in 57, 53, 41, and 31% yield as red crystals, respectively (Scheme 12). An exception was the reaction of η^1 -acetylide complex **17**, containing a sterically demanding *tert*-butyl group on the β -carbon atom, with the iminium ion **10**. The *tert*-butyl group prevents the addition on the β -carbon atom, and as a consequence, the η^1 -vinylidene complex **15** and enamine **2a** are formed by an acid–base reaction.

A further exception was the reaction of η^1 -acetylide complex **9** with iminium perchlorate **22**. After chromatography of the reaction mixture on silica gel with *n*-pentane/diethyl ether (10:0 to 10:3) in addition to the expected vinylcarbene complex **23**, isolated as orange crystals in 36% yield, the unsaturated aminocarbene complex **24** is obtained as an orange viscous oil with 14% yield (Scheme 13).

Starting from η^1 -vinylidene complex **25**, formed by aminoalkylation of **9** by **22**, two alternative pathways are conceivable for the formation of aminocarbene complex **24**. One possibility is the conversion of **25** by elimination of pyrrolidine to the allenylidene complex **26** and the nucleophilic attack of a pyrrolidine molecule to the electrophilic α -carbon atom of this intermediate (Scheme 14).¹⁷ Alternatively thermal 1,3-migration of pyrrolidine interconverts **25** in aminocarbene complex **24**.¹⁸ At the present time we have no indication for the



presence of allenylidene complex **26** in our reaction mixture, but β -elimination of H–X (water or amines) from vinylidene derivatives is a well-documented general method for the synthesis of transition metal allenylidene complexes.¹⁹ Judging by the isolated yield, the retro-ene reaction of **25** to **23** is the preferred reaction path.

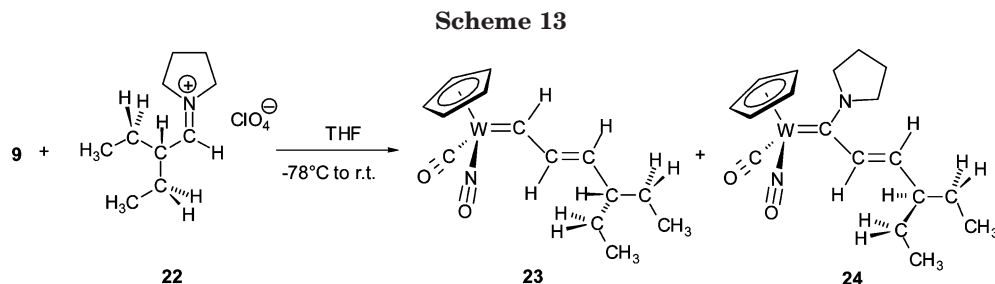
Characterization of 19, 20, 21, 23, and 24. The characterizations of **19**, **20**, **21**, and **23** are analogue to that for **3a–e**. Selected ^1H NMR and ^{13}C NMR signals of these complexes are presented in Table 1. The *trans* configuration of the vinyl moiety in **19** and **23** was discernible by the large $\text{H}_\beta\text{--H}_\gamma$ coupling constants (**19**, $J(\text{H}_\beta\text{--H}_\gamma) = 14.6$ Hz; **23**, $J(\text{H}_\beta\text{--H}_\gamma) = 14.5$ Hz).

The characterization of aminocarbene complex **24** was achieved by means of elemental analysis and standard spectroscopic techniques. The ^1H NMR spectroscopic as well as mass spectroscopic data and elemental analysis confirm the constitution of **24** as a 1:1 adduct of the acetylide complex **9** and iminium ion **22**. The most informative feature from the ^{13}C NMR spectrum of **24** is the signal for C_α at δ 250.9 ppm with the corresponding satellite signals caused by the coupling with the ^{183}W atom (14% ^{183}W abundance; $I = 1/2$), $^1J(\text{W--C}) = 126$ Hz.^{12b} The ^1H NMR spectra of **24** show a doublet at δ

(18) (a) Bibas, H.; Wong, M. W.; Wentrup, C. *Chem. Eur. J.* **1997**, *3*, 237. (b) Fulloon, B.; Wentrup, C. *J. Org. Chem.* **1996**, *61*, 1363.

(19) (a) Li, X.; Schopf, M.; Stephan, J.; Kippe, J.; Harms, K.; Sundemeyer, J. *J. Am. Chem. Soc.* **2004**, *126*, 8660. (b) Bruce, M. I. *Chem. Rev.* **1998**, *98*, 2797. (c) Fischer, E. O.; Kalder, H. J.; Frank, A.; Köhler, F. H.; Huttner, G. *Angew. Chem.* **1976**, *88*, 683; *Angew. Chem., Int. Ed. Engl.* **1976**, *15*, 623. (c) Berke, H. *Angew. Chem.* **1976**, *88*, 684; *Angew. Chem., Int. Ed. Engl.* **1976**, *15*, 624.

(17) Fischer, H.; Roth, G.; Reindl, D.; Troll, C. *J. Organomet. Chem.* **1993**, *454*, 133.

**Table 2. Crystal Data and Conditions for Crystallographic Data Collection and Structure Refinement of 3a and 4**

	3a	4
formula	C ₁₄ H ₁₇ NO ₂ W	C ₁₆ H ₂₁ N ₃ O ₂ W
fw	415.13	471.20
color	red, transparent	orange, transparent
cryst syst	monoclinic	monoclinic
space group	<i>P</i> 2 ₁ / <i>c</i>	<i>P</i> 2 ₁ / <i>c</i>
lattice constants	<i>a</i> = 12.730(1) Å, α = 90° <i>b</i> = 10.603(2) Å, β = 104.99(1)° <i>c</i> = 33.316(3) Å, γ = 90°	<i>a</i> = 12.399(2) Å, α = 90° <i>b</i> = 10.713(1) Å, β = 125.66(2)° <i>c</i> = 15.183(2) Å, γ = 90°
volume/Å ³	4344.00	1638.54
formula units per unit cell	<i>Z</i> = 4	<i>Z</i> = 4
density calc/g cm ⁻³	1.904	1.910
linear abs coeff/cm ⁻¹	79.7	70.6
diffractometer	Image Plate Diffractometer system (STOE)	
radiation	Mo K α	
monochromator	graphite	
2 θ range/deg	3.05° ≤ 2 θ ≤ 50.20° -15 ≤ <i>h</i> ≤ 15, -12 ≤ <i>k</i> ≤ 12 -39 ≤ <i>l</i> ≤ 39	3.81° ≤ 2 θ ≤ 56.30° -16 ≤ <i>h</i> ≤ 16, -12 ≤ <i>k</i> ≤ 14 -19 ≤ <i>l</i> ≤ 19
no. of reflns measd	26 054	14 405
no. of indep reflns	7501	3902
<i>R</i> _{int}	0.0739	0.0304
no. of indep reflns with <i>F</i> _o > 4 σ (<i>F</i> _o)	4414	3112
temperature/K	293	293
applied corrections, structure determination, and refinement	Lorenz and polarization coefficients <i>W</i> positional params from direct methods (SHELX-97); ^a further atoms from ΔF synthesis (SHELX-97); ^b refinement by anisotropic full-matrix least-squares procedure for all non-hydrogens, hydrogen atoms position refinement by "riding" model; atomic scattering factors from literature ^c	
no. of params	483	213
wR2	0.084	0.056
R1	0.069	0.035
R1 [<i>F</i> _o > 4 σ (<i>F</i> _o)]	0.033	0.023
max. and min. in $\Delta\sigma$ (e Å ⁻³)	0.86, -0.87	0.61, -0.75

^a Herrendorf, W. *HABITUS*, Program for numerical absorption correction; Universität Giessen, 1996. ^b Sheldrick, G. M. *SHELXS-97*, program for the Solution of Crystal Structures; Universität Göttingen, 1997. ^c Sheldrick, G. M. *SHELXL-97*, Program for Crystal Structure Refinement; Universität Göttingen, 1997. ^d *International Tables for Crystallography*; Wilson, A. J. C., Ed.; Kluwer Academic: Dordrecht, The Netherlands, 1992; Vol. C.

6.06 ppm with $J(\text{H}_\beta\text{-H}_\gamma) = 15.7$ Hz and a doublet of doublets at δ 5.08 ppm with $J(\text{H}_\beta\text{-H}_\gamma) = 15.8$ and 8.6 Hz characteristic of a *trans*-CH=CH-CH moiety. Due to the partial double-bond character, the rotation around the α -carbon atom and nitrogen atom is hindered and the ¹H NMR spectra of **24** show two sets of signals for the NCH₂ of the pyrrolidine ring. In the HMQC spectrum of **24** signals at δ 6.06 and 5.08 ppm in ¹H NMR spectrum show correlations to the signals at δ 138.8 and 138.4 ppm, respectively, in the ¹³C NMR spectrum, which are assigned to the β - and γ -carbon atoms. Significantly, the IR spectra of aminocarbene complex **24** exhibit a strong carbonyl band at 1894 cm⁻¹ and a strong nitrosyl band at 1575 cm⁻¹ in the range of similar aminocarbene complexes.¹² Comparison with the corresponding absorptions of the vinylcarbene complex **23**, $\tilde{\nu}(\text{CO})$ 1988 cm⁻¹ and $\tilde{\nu}(\text{NO})$ 1578 cm⁻¹, emphasizes the influence of the amino group. The large difference of the

absorption frequency of the carbonyl group in complex **23** compared to **24** indicates a better interaction of the amino group with the carbonyl ligand than with the nitrosyl group.

Crystal Structure of 3a. The structure of **3a** is further supported by a single-crystal X-ray diffraction study. Single crystals was obtained by slow diffusion of *n*-pentane in the dichloromethane solution of **3a** at -18 °C. The X-ray analysis shows three crystallographically independent molecular units. The units **I** and **II** are two stereoisomers of **3a**. Unit **III** could only be refined by an assumption of split positions for four carbon atoms of the cyclohexylidene ring with the ratio 0.5:0.5. The crystal parameters, data collection parameters, and conditions for structure refinement are summarized in Table 2. Three ORTEP diagrams of the molecular units are shown in Figure 1, and selected bond lengths and angles are given in Table 3. The W-C _{α} distance of

Table 3. Selected Bond Distances (Å) and Angles (deg) for Three Units of 3a and Calculated Values for 3Ma and 3Mb

unit I		unit II		unit III	
Distances					
W(1)–C(1)	2.018(11)	W(2)–C(15)	2.018(12)	W(3)–C(23)	1.993(12)
W(1)–N(1)	1.785(8)	W(2)–N(2)	1.772(10)	W(3)–N(3)	1.794(8)
W(1)–C(7)	1.976(9)	W(2)–C(21)	1.981(9)	W(3)–C(35)	1.988(9)
C(7)–C(8)	1.376(14)	C(21)–C(22)	1.440(12)	C(35)–C(36)	1.427(13)
C(8)–C(9)	1.356(13)	C(22)–C(23)	1.362(12)	C(36)–C(37)	1.334(12)
Angles					
C(1)–W(1)–N(1)	89.1(4)	C(15)–W(2)–N(2)	88.3(4)	C(29)–W(3)–N(3)	89.1(3)
C(1)–W(1)–C(7)	87.3(4)	C(15)–W(2)–C(21)	88.9(4)	C(29)–W(3)–C(35)	88.4(4)
N(1)–W(1)–C(7)	97.4(5)	N(2)–W(2)–C(21)	97.9(4)	N(3)–W(3)–C(35)	97.5(4)
W(1)–C(7)–C(8)	132.1(9)	W(2)–C(21)–C(22)	130.6(6)	W(3)–C(35)–C(36)	130.5(7)
C(7)–C(8)–C(9)	130.4(11)	C(21)–C(22)–C(23)	125.3(9)	C(35)–C(36)–C(37)	127.2(11)
3Ma			3Mb		
Distances					
W(2)–C(15)	2.026	W(2)–C(15)	2.027		
W(2)–N(2)	1.827	W(2)–N(2)	1.827		
W(2)–C(21)	2.019	W(2)–C(21)	2.009		
C(21)–C(22)	1.453	C(21)–C(22)	1.450		
C(22)–C(23)	1.352	C(22)–C(23)	1.351		
Angles					
C(15)–W(2)–N(2)	88.8	C(15)–W(2)–N(2)	88.8		
C(15)–W(2)–C(21)	88.6	C(15)–W(2)–C(21)	89.3		
N(2)–W(2)–C(21)	95.0	N(2)–W(2)–C(21)	95.9		
W(2)–C(21)–C(22)	129.5	W(2)–C(21)–C(22)	130.6		
C(21)–C(22)–C(23)	123.8	C(21)–C(22)–C(23)	124.0		
W(2)–C(21)–C(22)–C(23)	–179.4	W(2)–C(21)–C(22)–C(23)	–179.5		
N(2)–W(2)–C(21)–C(22)	–167.8	N(2)–W(2)–C(21)–C(22)	11.5		

1.971(10) Å in unit I, 1.981(9) Å in unit II, and 1.988(9) Å in unit III can be compared with the reported values in similar vinylcarbene tungsten complexes.^{11b} The X-ray analysis support an *s-trans* orientation of the diene unit. The angles between the planes formed by the atoms W, C_α, C_β and C_α, C_β, C_γ are 176° in unit I and 173° in unit II, consistent with the large H_α–H_β

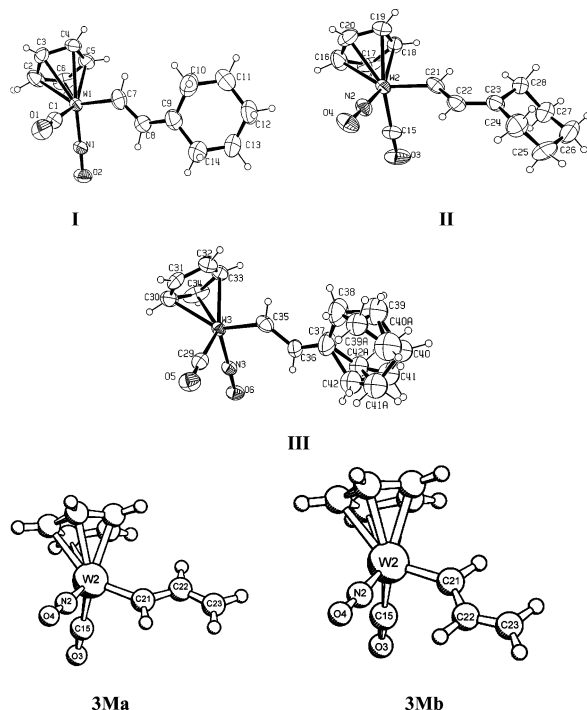


Figure 1. Molecular structure and atom-numbering scheme for units I–III of the experimental structure **3a** with H atoms and the calculated structures **3Ma** and **3Mb**. Thermal ellipsoids shown at the 30% probability level (ORTEP drawing).

Table 4. Selected Bond Distances (Å) and Angles (deg) of 4

Distances			
W–N(1)	1.780(3)	W–C(2)	2.365(4)
W–C(1)	1.953(4)	C(7)–N(2)	1.325(5)
W–C(7)	2.102(4)	C(7)–C(10)	1.520(4)
W–C(5)	2.317(6)	N(2)–C(8)	1.480(5)
W–C(4)	2.333(6)	C(8)–N(3)	1.444(5)
W–C(6)	2.357(5)	N(3)–C(9)	1.453(5)
W–C(3)	2.363(5)	C(9)–C(10)	1.559(6)
Angles			
N(1)–W–C(1)	92.24(18)	C(7)–N(2)–C(8)	123.6(3)
N(1)–W–C(7)	100.15(15)	C(11)–N(2)–C(8)	110.7(3)
C(1)–W–C(7)	89.89(16)	N(3)–C(8)–N(2)	111.4(3)
C(7)–W–C(2)	90.80(17)	C(8)–N(3)–C(9)	115.6(3)
N(2)–C(7)–C(10)	109.0(3)	C(9)–N(3)–C(14)	107.4(3)
N(2)–C(7)–W	129.5(3)	N(3)–C(9)–C(10)	111.08(18)
C(10)–C(7)–W	121.6(2)	C(7)–C(10)–C(9)	112.41(19)
C(7)–N(2)–C(11)	125.7(3)		

coupling constants (14.7 and 13.2 Hz, for two stereoisomers) in the ¹H NMR spectra of this complex. The C_β–C_γ bond lengths of 1.369(14) Å in unit I and 1.362(12) Å in unit II are in a typical range of a carbon–carbon double bond, and all the remaining values involving the alkyl group are as expected. Conspicuously the C_α–C_β distances show substantial differences among unit I (1.376(14) Å), unit II (1.440(12) Å), and unit III (1.427(13) Å).

Crystal Structure of 4. Suitable single crystals of complex **4** were obtained upon slow diffusion of *n*-pentane into a solution of **4** in dichloromethane at –18 °C under argon atmosphere. The X-ray diffraction study confirmed the structure of **4** as an asymmetric tricyclic aminocarbene complex. The crystal parameters, data collection parameters, and conditions for structure refinement are summarized in Table 2. Selected bonds distances and angles are given in Table 4. The ORTEP drawing with atomic numbering scheme is provided in

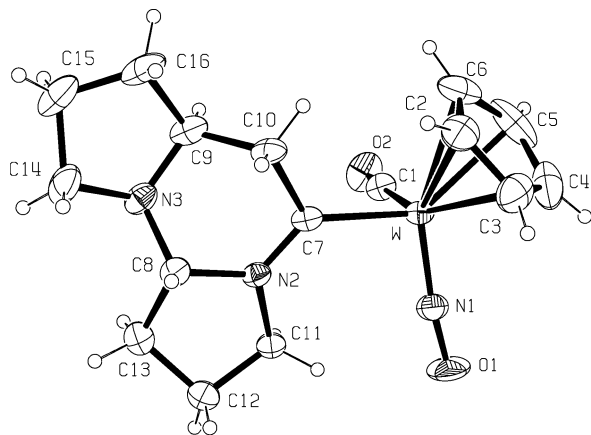


Figure 2. Molecular structure and atom-numbering scheme for **4** with H atoms. Thermal ellipsoids shown at the 30% probability level (ORTEP drawing).

Figure 2. The most notable features of the structure are bond angles around C(7) [C(10)–C(7)–W, 121.6(2)°; N(2)–C(7)–W, 129.5(2)°; C(10)–C(7)–N(2), 109.0(3)°; sum of angles 360°] and a W–C(7) distance of 2.102(4) Å that demonstrates the aminocarbene character of complex **4**.^{12a,20} The sum of angles around the N(2) atom (360.0°) and the C(7)–N(2) bond length of 1.325(4) Å reflect an sp^2 arrangement of the N(2) and considerable π -interaction between the N(2) and C(7). According to the X-ray analysis, the six-membered ring of **4** has a crystal boat conformation.

Kinetic Study. To obtain kinetic data for the retro-imino-ene reaction step, we measured the reaction rate of transformation of η^1 -vinylidene complex **6a** to vinylcarbene complex **3a**. Complex **6a** was prepared via the reaction of η^1 -acetylide complex **9** with iminium perchlorate **10** at -78 °C in THF- d_8 . The rate of reaction was measured by careful monitoring of the decay of the Cp resonance of **6a** (δ 6.05 and 6.02 ppm) using ^1H NMR spectroscopy. The formation of vinylcarbene complex **3a** resulting from retro-imino-ene reaction of **6a** (Scheme 5) was indicated by growth of the resonances of Cp protons of **3a** at δ 6.07 and 6.08 ppm, accompanied by diminution of the resonances of the Cp ligand of **6a**. The kinetic data were obtained at -16 , -6 , 4 , and 14 °C. Linear plots of $\ln([\mathbf{6a}]_0/[\mathbf{6a}]_t)$ versus time²¹ indicate that the retro-imino-ene reaction of **6a** is first order in the temperature range -16 to 14 °C. The first-order rate constants measured at four different temperatures are listed in Table 5. On the basis of the temperature dependence of k_{obs} , an activation energy E_a of 21.0 ± 1.4 kcal/mol was calculated. In Figure 3 is shown a plot of $\ln(k/T)$ vs $1/T$ (Eyring plot), from which ΔH^\ddagger , ΔS^\ddagger , and ΔG^\ddagger (at -1 °C) were found to be 20.5 ± 1.4 kcal/mol, -1.4 ± 0.6 cal/mol, and 20.9 ± 1.4 kcal/mol, respectively.

The observed activation energy E_a is substantially lower than the reported value for retro-ene reaction of substrates not containing a metallorganic component.

(20) (a) Dötz, K. H.; Naock, R.; Müller, G. *J. Chem. Soc., Chem. Commun.* **1988**, 302. (b) Parlier, A.; Rudler, H.; Daran, J. C.; Alvarez, C.; Delgado Reyers, F. *J. Organomet. Chem.* **1987**, 327, 339. (c) Dötz, K. H.; Fischer, H.; Hofmann, P.; Kreissl, F. R.; Schubert, U.; Weiss, K. *Transition Metal Carbene Complexes*; Verlag Chemie: Weinheim, 1983. (d) Casey, C. P.; Schusterman, A. J.; Vollendorf, N. W.; Haller, K. *J. Am. Chem. Soc.* **1982**, *104*, 2417.

(21) Wilkins, R. G. *Kinetics and Mechanisms of Reactions of Transition Metal Complexes*, 2nd ed.; VCH: Weinheim, Germany, 1991; p 13.

Table 5. First-Order Rate Constants of the Reaction of Intermediate η^1 -Vinylidene Complex **6a to **3a** in THF- d_8**

temp (°C)	$k/10^{-4} \text{ s}^{-1}$	r^a	temp (°C)	$k/10^{-4} \text{ s}^{-1}$	r^a
-16.0	0.142	0.986	4.0	2.710	0.988
-6.0	0.948	0.996	14.0	11.264	0.997

^a Correlation coefficient for the first-order plot.

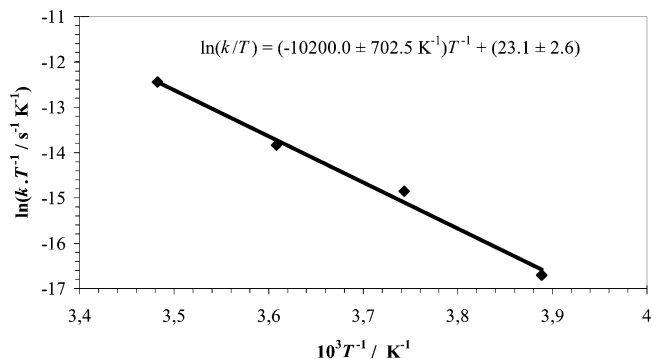
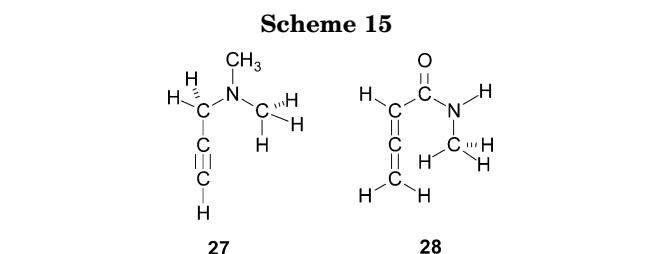
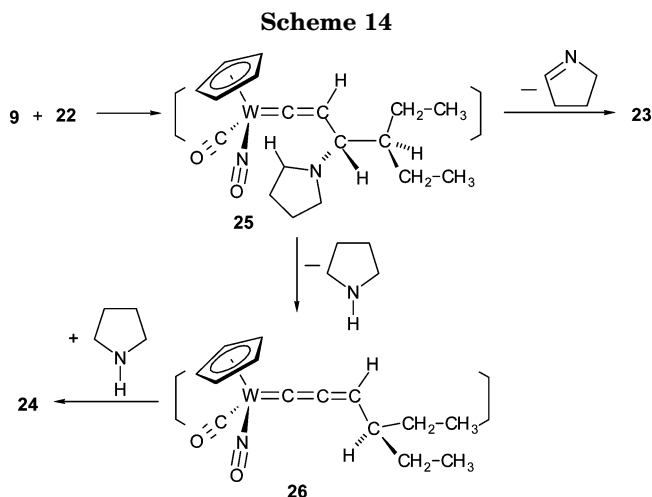


Figure 3. Plot of $\ln(k/T)$ vs $1/T$ based on observed reaction rates in THF- d_8 .



The experimental^{13b} and theoretically calculated²² activation energies are on the order of ~ 41 kcal/mol reported for the retro-ene reactions of propargylamines **27** and allenic amide **28**, respectively (Scheme 14). By considering the electronic features of the ligands on the tungsten atom of η^1 -vinylidene complex **6a**, the observed low activation energy for the retro-imino-ene reaction of **6a** is understandable. The electron-withdrawing nature of the ligands (CO and NO) on tungsten lowers the energy of the LUMO, which reduces the magnitude of the HOMO–LUMO energy separation in the transition state and thus increases the rate of the reaction.

Quantum Chemical Calculations. To further investigate the postulated reaction mechanism that is

(22) Bibas, H.; Koch, R.; Wentrup, C. *J. Org. Chem.* **1998**, *63*, 2619.

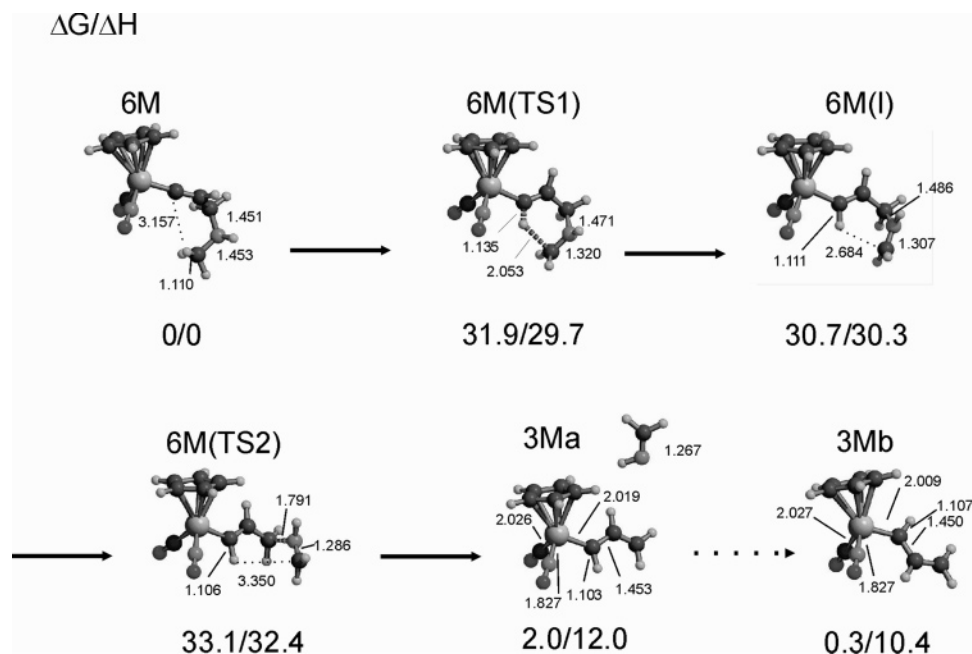


Figure 4. Calculated (B3LYP/TZ2P//B3LYP/SVP) reaction profile for the reaction **6M** → **3M**. Energy values in kcal/mol, distances in Å.

shown in Scheme 5, we calculated the reaction profile for the retro-imino-ene reaction of the model compound [(CO)(NO)(Cp)W=C=CH-CH₂-NH-CH₃] (**6M**), yielding [(CO)(NO)(Cp)W=CH-CH=CH₂] (**3M**) and methylene imine as reaction product, using density functional theory at the B3LYP level. The theoretically predicted reaction profile is given in Figure 4.

The calculations predict that the reaction **6M** → **3M** + CH₂NH proceeds with an activation barrier of $\Delta H^\ddagger = 32.4$ kcal/mol. The theoretical activation entropy is $\Delta S^\ddagger = -8.3$ cal/mol, which leads to ΔG^\ddagger (at -1 °C) = 33.1 kcal/mol. According to the calculated reaction profile, there is a shallow intermediate **6M(I)** that is formed after hydrogen migration from the terminal CH₃ group to the C_α carbon atom. The C_γ-N bond breaking reaction takes place in the second part of the two-step reaction. Note that the transition state **6M(TS1)** for the hydrogen migration step is energetically lower-lying than the intermediate **6M(I)** when the zero-point vibrational corrections and thermal contributions are considered. This means that the process is more likely a single-step reaction where the hydrogen migration and carbon-nitrogen bond breaking appear as two consecutive reactions but without formation of a true intermediate. The calculated energies for the reaction profile of the model compound are somewhat higher than the experimental values. We think that the difference comes from the use of the model substituent in the calculations instead of the bulky groups that are employed in the experimental work.

The calculated reaction **6M** → **3M** + CH₂NH yields structure **3Ma** as an isomer of the tungsten carbene complex. We searched for other isomers and optimized the geometries of different forms of **3M**. The geometry optimization gave **3Mb** as a second isomer, which is 1.6 kcal/mol lower in energy than **3Ma**. The reaction **6M** → **3M** (**a** or **b**) + CH₂NH at -1 °C is slightly endergonic ($\Delta G = 0.3$ kcal/mol for **3Ma** and $\Delta G = 2.0$ kcal/mol for **3Mb**). Note that the enthalpy contribution to the thermodynamics of the reaction is rather large.

The most important bond lengths and bond angles of **3Ma** and **3Mb** are shown in Table 3. A comparison of the calculated data with the experimental values for units **I–III** of **3a** shows that the bond angles agree quite well, while the calculated tungsten-ligand distances are slightly longer than the theoretical values. This is partly caused by solid-state effects, which tend to shorten donor-acceptor distances.²³ We want to point out that the calculated C-C distances of **3Ma** and **3Mb** are in excellent agreement with the experimental data for **II** but not with **I** and **III**. The calculated C_α-C_β distances (1.450 and 1.453 Å) agree with the experimental value of unit **II** (1.440(12) Å), while they are clearly longer than in unit **I** (1.376 Å) and somewhat longer than in unit **III** (1.427 Å).

Experimental Section

General Considerations. All reactions were carried out under an argon atmosphere (99.99%, by Messer-Griesheim) with the use of standard Schlenk techniques. Solvents were purified by standard methods and distilled under argon prior to use. Literature methods were used to prepare [(η⁵-C₅H₅)(CO)(NO)W=C=CHR] (**1**, **14**, **15**),^{16b} enamines **2a–e**,²⁴ and iminiums **10**, **11**, **13**, **18**, and **22**.²⁵ All other compounds were commercially available. NMR spectra were obtained on a Bruker AM 400 spectrometer (¹H NMR, 400.13 MHz; ¹³C NMR, 100.61 MHz). Proton and carbon chemical shifts are reported in ppm relative to the residual proton resonance (7.24 ppm) or the carbon multiplet (77.0 ppm) of the NMR solvent CDCl₃. ¹³C DEPT experiments were run on a Bruker AM 400 spectrometer. MS measurements (70 eV) were performed on a Varian MAT 311-A. IR spectra were recorded on a Bruker FT-IR IFS 85. UV/vis spectra were recorded on Hewlett-Packard 8452 spectrometers. Microanalyses were performed on a Carlo Erba 1104 elemental analyzer.

(23) Jonas, V.; Frenking, G.; Reetz, M. T. *J. Am. Chem. Soc.* **1994**, *116*, 8741.

(24) (a) Carlson, R.; Nilsson, Å. *Acta Chem. Scand. B* **1984**, *38*, 49 (b) Carlson, R.; Nilsson, Å.; Strömqvist, M. *Acta Chem. Scand. B* **1983**, *37*, 7 (c) Stork, G.; Brizzolara, A.; Landesman, H.; Szmuszkovics, J.; Terrell, R. *J. Am. Chem. Soc.* **1963**, *85*, 207.

(25) Leonard N. J.; Paukstelis, J. V. *J. Org. Chem.* **1963**, *28*, 3021.

General Synthesis of Vinylcarbene Complexes 3a–e.

All the complexes were prepared by the process described below. At room temperature a solution of 1.5 mmol of enamines **2a–d** in 2 mL of THF was added dropwise to a solution of 0.5 g (1.5 mmol) of η^1 -vinylidene complex **1** in 10 mL of THF, whereby the color changed from orange to deep red. After the reaction mixture was stirred for 1–2 h, the THF was removed under reduced pressure. Chromatography on silica gel with *n*-pentane/diethyl ether (10:1) gave vinylcarbene complexes **3a–d** as red crystals. The synthesis of vinylcarbene complex **3e** is analogue to that for **3a–d**; instead of 1.5 mmol of enamine, 1.5 mmol of η^1 -vinylidene complex **1** was treated with 4.5 mmol of enamine **2e** and the reaction mixture was stirred for 12 h. Chromatography gave complex **3e** as red crystals and complex **6** as orange crystals.

[(η^5 -C₅H₅)(CO)(NO)W(*trans*- (=CHCH=C-CH₂-(CH₂)₃-CH₂)] (3a). The product was recrystallized from diethyl ether/*n*-pentane, giving a crystalline red solid, 54% yield. Anal. Calcd for C₁₄H₁₇WNO₂: C, 40.50; H, 4.12; N, 3.37. Found: C, 40.07; H, 3.90; N, 3.44. Two rotamers (8:1) were found in the ¹H NMR spectra. ¹H NMR (CDCl₃): δ 15.03 and 14.20 (two d, 1:8, $J_{H-H} = 14.7$ Hz and $J_{H-H} = 13.2$ Hz, 1H, H _{α}), 8.04 and 7.21 (two d, 8:1, $J_{H-H} = 13.2$ Hz and $J_{H-H} = 14.7$ Hz, H _{β}), 5.91 and 5.90 (two s, 8:1, 5H, Cp), 2.28–1.94 (m, 4H, (-CH₂-(CH₂)₃-CH₂-)), 1.74–1.44 (m, 6H, (-CH₂-(CH₂)₃-CH₂-)); ¹³C NMR (CDCl₃) δ 274.4 (C _{α}), 214.2 (CO), 144.5 (C _{γ}), 142.7 and 142.0 (C _{β}), 97.2 and 96.3 (C _{ρ}), 38.3, 37.8, 30.4, 30.2, 28.5, 28.3, 27.7, 26.8 (-CH₂-(CH₂)₃-CH₂-). IR (KBr): $\tilde{\nu}$ (CO) 1981 cm⁻¹, $\tilde{\nu}$ (NO) 1586 and 1567 cm⁻¹; IR (CaF₂; -64°C; solution in THF): $\tilde{\nu}$ (CO) 1973 cm⁻¹, $\tilde{\nu}$ (NO) 1606 and 1575 cm⁻¹. MS (70 eV): *m/e* 415 (M⁺, ¹⁸⁴W), 387 (M⁺ - CO); high-resolution mass spectrum calcd for C₁₄H₁₇¹⁸²WNO₂ (M⁺) *m/e* 413.0741, found *m/e* 413.0743. UV/vis (20 °C): λ_{\max} (log ϵ ; solvent) = 374 (3.913, THF), shoulder at 340 nm.

[(η^5 -C₅H₅)(CO)(NO)W(*trans*- (=CHCH=C-CH₂-(CH₂)₂-CH₂)] (3b). The product was recrystallized from diethyl ether/*n*-pentane, giving a crystalline red solid, 51% yield. Anal. Calcd for C₁₃H₁₅WNO₂: C, 38.92; H, 3.76; N, 3.49. Found: C, 39.27; H, 4.04; N, 3.34. Two rotamers (7:1) were found in the ¹H NMR spectra. ¹H NMR (CDCl₃): δ 14.68 and 13.87 (two d, 1:7, $J_{H-H} = 14.8$ Hz and $J_{H-H} = 13.2$ Hz, 1H, H _{α}), 8.18 and 7.35 (two d, 7:1, $J_{H-H} = 13.2$ Hz and $J_{H-H} = 14.8$ Hz, 1H, H _{β}), 5.93 and 5.92 (two s, 7:1, 5H, Cp), 2.12–2.03 (m, 4H, (-CH₂-(CH₂)₂-CH₂-)), 1.76–1.64 (m, 4H, (-CH₂-(CH₂)₂-CH₂-)). ¹³C NMR (CDCl₃): δ 276.3 (C _{α}), 214.3 (CO), 150.0 (C _{γ}), 141.7 and 141.0 (C _{β}), 97.3 and 97.1 (C _{ρ}), 34.7, 34.5, 31.1, 30.8, 25.9, 25.8, 25.7 (-CH₂-(CH₂)₂-CH₂-). IR (KBr): $\tilde{\nu}$ (CO) 1965 cm⁻¹, $\tilde{\nu}$ (NO) 1571 and 1561 cm⁻¹. MS (70 eV): *m/e* 401 (M⁺, ¹⁸⁴W), 373 (M⁺ - CO); high-resolution mass spectrum calcd for C₁₃H₁₅¹⁸²WNO₂ (M⁺) *m/e* 399.0585, found *m/e* 399.0591.

[(η^5 -C₅H₅)(CO)(NO)W(*trans*- (=CHCH=C(CH₂CH₃)] (3c). The product was recrystallized from diethyl ether/*n*-pentane, giving a crystalline red solid, 60% yield. Anal. Calcd for C₁₃H₁₇WNO₂: C, 38.73; H, 4.25; N, 3.47. Found: C, 38.34; H, 4.27; N, 3.20. Two rotamers (7:1) were found in the ¹H NMR spectra. ¹H NMR (CDCl₃): δ 14.93 and 14.10 (two d, 1:7, $J_{H-H} = 14.7$ Hz and $J_{H-H} = 13.1$ Hz, 1H, H _{α}), 7.98 and 7.14 (two d, 7:1, $J_{H-H} = 13.1$ Hz and $J_{H-H} = 14.7$ Hz, 1H, H _{β}), 5.84 and 5.83 (two s, 7:1, 5H, Cp), 2.13–1.91 (m, 4H, CH₂), 1.05 (t, $J_{H-H} = 7.5$ Hz, 3H, CH₃), 0.90 and 0.89 (two t, 1:7, $J_{H-H} = 7.5$ Hz and $J_{H-H} = 7.6$ Hz, 3H, CH₃). ¹³C NMR (CDCl₃): δ 275.2 (C _{α}), 214.0 (CO), 147.3 (C _{γ}), 143.5 ($^2J(^{183}\text{W}-^{13}\text{C}) = 5.1$ Hz) and 142.6 (C _{β}), 97.5 and 97.3 (C _{ρ}), 30.6, 30.4, 24.8, 24.5 (CH₂), 13.2, 13.1, 12.1 (CH₃). IR (KBr): $\tilde{\nu}$ (CO) 1978 cm⁻¹, $\tilde{\nu}$ (NO) 1596 and 1575 cm⁻¹. MS (70 eV): *m/e* 403 (M⁺, ¹⁸⁴W), 375 (M⁺ - CO); high-resolution mass spectrum calcd for C₁₃H₁₇¹⁸²WNO₂ (M⁺) *m/e* 401.07415, found *m/e* 401.0769.

[(η^5 -C₅H₅)(CO)(NO)W(*trans*- (=CHCH=C(CH₂CH(CH₃)₂)] (3d). The product was recrystallized from diethyl ether/*n*-pentane, giving a crystalline red solid, 50% yield. Anal. Calcd for C₁₇H₂₅WNO₂: C, 44.46; H, 5.48; N 3.05. Found: C,

44.10; H, 5.72; N, 2.62. Two rotamers (30:1) were found in the NMR spectra. ¹H NMR (CDCl₃): δ 14.95 and 14.07 (two d, 1:30, $J_{H-H} = 12.0$ Hz and $J_{H-H} = 13.1$ Hz, 1H, H _{α}), 8.04 and 7.26 (two d, 30:1, $J_{H-H} = 13.1$ Hz and $J_{H-H} = 12.0$ Hz, 1H, H _{β}), 5.84 and 5.82 (two s, 30:1, 5H, Cp), 1.85–1.75 (m, 5H, two CH₂ and one CH), 1.71–1.61 (m, 1H, CH), 0.84–0.75 (m, 12 H, CH₃). ¹³C NMR (CDCl₃): δ 275.5 (C _{α}), 214.0 (CO), 147.3 (t, $^2J(^{183}\text{W}-^{13}\text{C}) = 5.1$ Hz) and 146.6 (C _{β}), 142.3 (C _{γ}), 97.5 and 97.2 (C _{ρ}), 48.0, 47.5, 40.6, 40.5 (CH₂), 27.3, 26.6 (CH), 23.0, 22.9, 22.8, 22.7, 22.6, 22.5, 22.3 (CH₃). IR (KBr): $\tilde{\nu}$ (CO) 1989 and 1976 cm⁻¹, $\tilde{\nu}$ (NO) 1568 and 1562 cm⁻¹. MS (70 eV): *m/e* 459 (M⁺, ¹⁸⁴W), 431 (M⁺ - CO); high-resolution mass spectrum calcd for C₁₇H₂₅¹⁸²WNO₂ (M⁺) *m/e* 457.1367, found *m/e* 457.1383.

[(η^5 -C₅H₅)(CO)(NO)W(*trans*- (=CHCH=C(CH(CH₃)₂)] (3e). The product was recrystallized from diethyl ether/*n*-pentane, giving a crystalline red solid, 37% yield. Anal. Calcd for C₁₅H₂₁WNO₂: C, 41.78; H, 4.91; N, 3.25. Found: C, 41.33; H, 4.72; N, 3.70. Two rotamers (15:1) were found in the NMR spectra. ¹H NMR (CDCl₃): δ 15.12 and 14.29 (two d, 1:15, $J_{H-H} = 12.0$ Hz and $J_{H-H} = 13.2$ Hz, 1H, H _{α}), 8.11 and 7.28 (two d, 15:1, $J_{H-H} = 13.2$ Hz and $J_{H-H} = 12.0$ Hz, 1H, H _{β}), 5.91 and 5.89 (two s, 15:1, 5H, Cp), 3.19–3.12 and 3.04–2.93 (two m, 1:15, 1H, CH), 2.50–2.40 (m, 1H, CH), 1.14, 1.13, 1.09, and 1.08 (four d, 15:15:1:1, $J_{H-H} = 7.0$ Hz, $J_{H-H} = 7.3$ Hz, $J_{H-H} = 6.9$ Hz and $J_{H-H} = 7.0$ Hz, 6H, CH₃), 1.01 and 1.00 (two d, 1:1, $J_{H-H} = 6.9$ Hz, $J_{H-H} = 6.9$ Hz, 6H, CH₃); ¹³C NMR (CDCl₃) δ 274.5 (C _{α}), 214.2 (t, $^1J(^{183}\text{W}-^{13}\text{C}) = 102.5$ Hz) and 214.7 (CO), 154.8 and 154.9 (C _{γ}), 141.7 (t, $^2J(^{183}\text{W}-^{13}\text{C}) = 9.8$ Hz) and 140.7 (C _{β}), 97.5 and 97.3 (C _{ρ}), 30.4, 30.3, 29.8, 29.4 (CH), 23.4, 23.3, 23.2, 20.8, 20.7, 20.5, 20.4 (CH₃). IR (KBr): $\tilde{\nu}$ (CO) 1968 cm⁻¹, $\tilde{\nu}$ (NO) 1594 and 1564 cm⁻¹. MS (70 eV): *m/e* 431 (M⁺, ¹⁸⁴W), 403 (M⁺ - CO); high-resolution mass spectrum calcd for C₁₅H₂₁¹⁸²WNO₂ (M⁺) *m/e* 429.1054, found *m/e* 429.1084.

Tricyclic Aminocarbene Complex 4. The product was recrystallized from CH₂Cl₂/*n*-pentane, giving a crystalline orange solid, 12% yield. Anal. Calcd for C₁₆H₂₁WN₃O₂: C, 40.78; H, 4.49; N, 8.92. Found: C, 40.98; H, 4.12; N, 8.50. ¹H NMR (CDCl₃): δ 5.59 (s, 5H, Cp), 4.00–3.78 (m, 4H, NCH₂), 3.61–3.35 (m, 4H, two CH and CH₂), 2.14–1.72 (8H, four CH₂). ¹³C NMR (CDCl₃): δ 251.0 (C _{α}), 235.2 (CO), 133.15 (C _{ρ}), 93.9 (C _{ρ}), 66.6 (C₉), 59.9 (C₁₄), 47.4 (C₁₁), 45.5 (C₁₀), 37.6 (C₁₃), 26.2 (C₁₆), 26.0 (C₁₅), 24.6 (C₁₂). IR (KBr): $\tilde{\nu}$ (CO) 1899 cm⁻¹, $\tilde{\nu}$ (NO) 1560 cm⁻¹.

[(η^5 -C₅H₅)(CO)(NO)W(*trans*- (=CHCD=C-CHD-(CH₂)₂-CH₂)] (8). The preparation of **8** is analogous to that for **3b**; instead of η^1 -vinylidene complex **1**, η^1 -vinylidene complex **1-D** was used. The product was recrystallized from diethyl ether/*n*-pentane, giving a crystalline red solid, 52% yield. Anal. Calcd for C₁₃H₁₃D₂WNO₂: C, 38.73; H, 3.75; N, 3.47. Found: C, 39.16; H, 3.34; N, 3.18. ¹H NMR (CDCl₃): δ 14.65 and 13.83 (two s, 1:10, 1H, H _{α}), 5.91 and 5.89 (two s, 1:4, 5H, Cp), 2.12–2.03 (m, 3H, (-CHD-(CH₂)₂-CH₂-)), 1.76–1.64 (m, 4H, (-CHD-(CH₂)₂-CH₂-)); ¹³C NMR (CDCl₃): δ 276.2 (C _{α}), 214.3 (CO), 149.8 (C _{γ}), 141.6 and 141.0 (C _{β}), 97.3 and 97.1 (C _{ρ}), 34.7, 34.4, 31.1, 30.8, 25.9, 25.8, 25.7 (-CH₂-(CH₂)₂-CH₂-). IR (KBr): $\tilde{\nu}$ (CO) 1965 cm⁻¹, $\tilde{\nu}$ (NO) 1568 cm⁻¹. MS (70 eV): *m/e* 403 (M⁺, ¹⁸⁴W), 375 (M⁺ - CO); high-resolution mass spectrum calcd for C₁₃H₁₃D₂¹⁸²WNO₂ (M⁺) *m/e* 401.0708, found *m/e* 401.0680.

General Synthesis of Vinylcarbene Complexes 3a, 19–21, and 23 and Aminocarbene Complex 24. All the complexes were prepared by the process described below. At -78 °C 1 mL (1.5 mmol) of *n*-C₄H₉-Li (a solution of 1.5 mmol/mL) in hexane was added to a solution of 0.50 g (1.5 mmol) of η^1 -vinylidene complex **1** in 15 mL of THF. The color of solution changed immediately from orange to deep green. Addition of 1.5 mmol of iminium salts **10**, **11**, **13**, and **18** under argon atmosphere to the deep green solution of η^1 -acetylide complex **9** led to a dark red solution. After the reaction mixture was allowed to reach room temperature, the THF was removed under reduced pressure. Chromatography of the residue on silica gel with *n*-pentane/diethyl ether (10:1) gave vinylcarbene

complexes **3a**, **21**, and **19** as red crystals. The preparation of vinylcarbene complex **20** is analogue to that for **3a**, **19**, and **21**; instead of η^1 -vinylidene complex **1**, 0.61 g (1.5 mmol) of η^1 -vinylidene complex **14** was used. The reaction of η^1 -acetylide complex **9** with iminium salt **22** is analogous to that for **10**, **11**, **13**, and **18**. Chromatography gave vinylcarbene complex **23** as red crystals and aminocarbene complex **24** as a red oil.

[(η^5 -C₅H₅)(CO)(NO)W(*trans*- (=CHC(Ph)=C-CH₂-CH₂)₃-CH₂)] (20**).** The product was recrystallized from diethyl ether/*n*-pentane, giving a crystalline red solid, 31% yield. Anal. Calcd for C₂₀H₂₁WNO₂: C, 48.90; H, 4.30; N, 2.85. Found: C, 48.83; H, 3.95; N, 3.05. ¹H NMR (CDCl₃): δ 15.47 and 14.38 (two s, 1:8, 1H, H_a), 7.43–7.09 (m, 5H, Ph), 5.88 and 5.21 (two s, 8:1, 5H, Cp), 2.55–2.31 (m, 2H, CH₂), 1.90–1.45 (m, 8H, CH₂). ¹³C NMR (CDCl₃): δ 273.7 and 273.4 (C_a), 215.0 and 214.9 (CO), 152.8 (C _{β}), 145.1 and 143.7 (C _{γ}), 142.3 (C_{ipso}), 130.6, 129.6, 128.3, 126.4, 125.8 (arom C), 97.5 and 97.0 (Cp), 34.3, 34.0, 32.7, 32.4, 28.5, 28.3, 26.7, 26.6 (CH₂). IR (KBr): $\bar{\nu}$ (CO) 1993 cm⁻¹, $\bar{\nu}$ (NO) 1597 cm⁻¹. MS (70 eV): *m/e* 491 (M⁺, ¹⁸⁴W), 463 (M⁺ – CO); high-resolution mass spectrum calcd for C₂₀H₂₁¹⁸²WNO₂ (M⁺) *m/e* 489.1054, found *m/e* 489.1027.

[(η^5 -C₅H₅)(CO)(NO)W(*trans*- (=CHCH=C(CH₃)₂)] (21**).** The product was recrystallized from diethyl ether/*n*-pentane, giving a crystalline red solid, 53% yield. Anal. Calcd for C₁₁H₁₃WNO₂: C, 35.22; H, 3.49; N, 3.73. Found: C, 35.04; H, 3.20; N, 3.64. ¹H NMR (CDCl₃): δ 14.91 and 14.07 (two d, 1:15, J_{H-H} = 12.0 Hz and J_{H-H} = 12.0 Hz, 1H, H_a), 8.10, 8.06 and 7.26 (three m, 15:15:1, 1H, H _{β}), 5.92 and 5.90 (two s, 15:1, 5H, Cp), 1.68, 1.66, 1.64, 1.58 (four s, 15:1:1:15, 6H, CH₃). ¹³C NMR (CDCl₃): δ 274.9 (C_a), 214.0 (CO), 145.8 and 145.1 (C _{β}), 136.6 (C _{γ}), 97.4 and 97.2 (Cp), 26.5, 26.6, 19.4 (CH₃). IR (KBr): $\bar{\nu}$ (CO) 1971 cm⁻¹, $\bar{\nu}$ (NO) 1598 and 1576 cm⁻¹. MS (70 eV): *m/e* 375 (M⁺, ¹⁸⁴W), 347 (M⁺ – CO); high-resolution mass spectrum calcd for C₁₁H₁₃¹⁸²WNO₂ (M⁺) *m/e* 373.0428, found *m/e* 373.0401.

[(η^5 -C₅H₅)(CO)(NO)W(*trans*- (=CHCH=CHCH(CH₃)₂)] (19**).** The product was recrystallized from diethyl ether/*n*-pentane, giving a crystalline red solid, 41% yield. Anal. Calcd for C₁₂H₁₅WNO₂: C, 37.04; H, 3.88; N, 3.59. Found: C, 37.35; H, 3.51; N, 3.83. ¹H NMR (CDCl₃): δ 14.51(d) and 13.72 (d, J_{H-H} = 12.3 Hz) (1:23, 1H, H_a), 8.05 (dd, J_{H-H} = 12.3 and 14.6 Hz) and 7.20 (23:1, H _{β}), 5.94 and 5.91 (two s, 1:23, 5H, Cp), 5.64 (dd, J_{H-H} = 14.6 Hz and J_{H-H} = 7.4 Hz, 1H, H _{γ}), 2.27 (m, 1H, CH), 1.08 and 1.06 (two d, J_{H-H} = 6.49 Hz, 1:1, 6H, CH₃). ¹³C NMR (CDCl₃): δ 283.5 (C_a), 213.2 (CO), 146.2 (t, ²J(¹⁸³W–¹³C) = 6 Hz) and 145.6 (C _{β}), 144.0 and 143.5 (t, ³J(¹⁸³W–¹³C) = 4.6 Hz), (C _{γ}), 97.5 and 97.4 (Cp), 31.1 (CH), 21.6, 21.5 (CH₃). IR (KBr): $\bar{\nu}$ (CO) 1986 cm⁻¹, $\bar{\nu}$ (NO) 1575 cm⁻¹. MS (70 eV): *m/e* 389 (M⁺, ¹⁸⁴W), 361 (M⁺ – CO); high-resolution mass spectrum calcd for C₁₂H₁₅¹⁸²WNO₂ (M⁺) *m/e* 387.0586, found *m/e* 387.0574.

[(η^5 -C₅H₅)(CO)(NO)W(*trans*- (=CHCH=CHCH-(CH₂CH₃)₂)] (23**).** The product was recrystallized from diethyl ether/*n*-pentane, giving a crystalline red solid, 36% yield. Anal. Calcd for C₁₄H₁₉WNO₂: C, 40.30; H, 4.59; N, 3.35. Found: C, 40.22; H, 4.31; N, 3.57. ¹H NMR (CDCl₃): δ 13.72 (d) and 14.60 (d, J_{H-H} = 12.3 Hz) (1:30, 1H, H_a), 8.01 (dd, J_{H-H} = 12.3 Hz and J_{H-H} = 14.5 Hz, 1H, H _{β}), 5.92 and 5.90 (two s, 30:1, 5H, Cp), 5.45 (dd, J_{H-H} = 14.54 Hz and J_{H-H} = 9.83 Hz, 1H, H _{γ}), 1.83 (m, 1H, CH), 1.56–1.24 (m, 4H, CH₂), 0.90–0.83 (m, 6H, CH₃). ¹³C NMR (CDCl₃): δ 283.2 (C_a), 213.2 (CO), 149.1 and 148.6 (C _{β}), 141.8 and 141.3 (C _{γ}), 97.4 (Cp), 46.2 and 45.9 (CH), 27.5, 27.0, 26.8, 26.7 (CH₂), 11.8 and 11.7 (CH₃). IR (KBr): $\bar{\nu}$ (CO) 1988 cm⁻¹, $\bar{\nu}$ (NO) 1578 cm⁻¹. MS (70 eV): *m/e* 417 (M⁺, ¹⁸⁴W), 389 (M⁺ – CO); high-resolution mass spectrum calcd for C₁₄H₁₉¹⁸²WNO₂ (M⁺) *m/e* 415.0898, found *m/e* 387.0888.

Aminocarbene complex 24: orange oil, 14% yield. Anal. Calcd for C₁₈H₂₆WN₂O₂: C, 44.46; H, 5.39; N, 5.75. Found: C, 44.21; H, 5.58; N, 5.91. ¹H NMR (CDCl₃): δ 6.06 (d, J_{H-H} = 15.7 Hz, 1H, H _{β}), 5.44 (s, 5H, Cp), 5.08 (dd, J_{H-H} = 15.8 Hz and J_{H-H} = 8.6 Hz, 1H, H _{γ}), 3.95–3.73 (m, 2H, NCH₂), 3.46 (t, J_{H-H} = 6.8 Hz, 2H, NCH₂), 2.09–1.91 (m, 4H, CH₂CH₂),

1.82–1.71 (m, 1H, CH), 1.45–1.12 (m, 4H, CH₂), 0.82 and 0.79 (two t, J_{H-H} = 7.4 Hz and J_{H-H} = 7.4 Hz, 6H, CH₃). ¹³C NMR (CDCl₃): δ 250.9 (t, ¹J(¹⁸³W–¹³C) = 126 Hz, C_a), 234.3 (CO), 138.8 (C _{β}), 138.4 (C _{γ}), 93.9 (Cp), 58.8 and 53.1 (NCH₂), 46.3 (CH), 27.4 and 26.8 (CH₂), 26.2 and 25.3 (NCH₂CH₂), 11.9 and 11.5 (CH₃). IR (KBr): $\bar{\nu}$ (CO) 1894 cm⁻¹, $\bar{\nu}$ (NO) 1575 cm⁻¹. MS (70 eV) *m/e* 486 (M⁺, ¹⁸⁴W), 458 (M⁺ – CO); high-resolution mass spectrum calcd for C₁₈H₂₆¹⁸²WNO₂ (M⁺) *m/e* 484.1476, found *m/e* 484.1467.

Monitoring of the Reaction of η^1 -Acetylide Complex 9 with Iminium 10 by IR and UV/Vis Spectroscopy. At –78 °C to a solution of 0.50 g (1.5 mmol) of η^1 -vinylidene complex **1** under argon atmosphere was added 1 mL (1.5 mmol) of *n*-C₄H₉-Li (a solution of 1.5 mmol/mL) in hexane; the color of the reaction solution changed immediately from orange to green. A small amount of reaction solution was transferred rapidly via a channel to an CaF₂ IR-cell at –64 °C and an IR spectrum was recorded. Additionally, to the deep green solution was added 0.38 g (1.5 mmol) of iminium salt **10**, and an IR spectrum was recorded every 20 min. After 2 h the reaction mixture was annealed slowly to room temperature, and an IR spectrum was recorded every 20 min at –64 °C. From an analogous process, the reaction was monitored with UV/vis spectroscopy. IR (CaF₂, THF, –64 °C): η^1 -acetylide complex **9**, $\bar{\nu}$ (CO) 1864 cm⁻¹, $\bar{\nu}$ (NO) 1460 cm⁻¹; η^1 -vinylidene complex **6a**, $\bar{\nu}$ (CO) 1986 cm⁻¹, $\bar{\nu}$ (NO) 1643 and 1614 cm⁻¹; vinylcarbene complex **3a**, $\bar{\nu}$ (CO) 1973 cm⁻¹, $\bar{\nu}$ (NO) 1606 and 1575 cm⁻¹. UV/vis (THF, –78 °C): η^1 -acetylide complex **9**, λ_{\max} = 606 nm (log ϵ = 1.574); η^1 -vinylidene complex **6a**, λ_{\max} = 454 nm (log ϵ = 2.127) and 309 (log ϵ = 3.812) and a shoulder at 363; vinylcarbene complex **3a**, λ_{\max} = 374 nm (log ϵ = 4.114) and a shoulder at 340 nm.

Monitoring of the Reaction of η^1 -Acetylide Complex 9 with Iminium Ion 11 by NMR Spectroscopy. In a NMR tube the hexane of 0.1 mL of *n*-C₄H₉-Li in hexane (1.5 mmol/mL) was evaporated under high vacuum. To the yellow oily residue was added at –78 °C a solution of 50 mg (0.15 mmol) of complex **1** in 0.8 mL of THF-*d*₈. After shaking the reaction mixture, the color changed to deep clear green. To this green solution was added under argon atmosphere 32 mg (0.15 mmol) of iminium salt **11**. The reaction mixture was shaken every 15 min. After 2 h the ¹H NMR, ¹³C NMR, and HMQC spectra were recorded at –70 °C. ¹H NMR (THF-*d*₈, –70 °C): δ 6.05 and 6.03 (two s, 1:1, 5H, Cp), 5.68 and 5.67 (two s, 1:1, 1H, C _{β} H), 2.69–2.57 (m, 4H, NCH₂), 1.69–1.66 (m, 4H, CH₂), 1.14 and 1.10 (two s, 1:1, 6H, CH₃). ¹³C NMR (THF-*d*₈, –70 °C): δ 336.0 and 334.7 (two t, ¹J(¹⁸³W–¹³C) = 186 and 182 Hz, C_a), 216.0 and 215.1 (CO), 128.6 and 127.8 (C _{β}), 97.6 and 97.5 (Cp), 59.4 and 57.8 (C), 47.2, 47.0 (NCH₂), 29.8 and 29.4 (CH₃), 24.8 and 24.5 (CH₂).

Kinetic Study of the Reaction of Intermediate 6a to 3a in THF-*d*₈. A typical experiment was done in the following way. In a NMR tube the hexane of 0.1 mL of *n*-C₄H₉-Li in hexane (1.5 mmol/mL) was evaporated under high vacuum. To a yellow oily residue was added at –78 °C a solution of 50 mg (0.15 mmol) of complex **1** in 0.8 mL of THF-*d*₈. After shaking the reaction mixture, the color changed to deep clear green. To this green solution was added under argon atmosphere 32 mg (0.15 mmol) of iminium salt **10**. The reaction mixture was shaken every 15 min. After 2 h the NMR tube was then placed into a thermostat at a fixed temperature. At regular time intervals, the tube was removed and the reaction quenched at –78 °C. The reaction time was followed by measuring the relative peak integration of the ¹H NMR of the cyclopentadienyl signals of **3a** (δ 6.07 and 6.08 ppm) and **6a** (δ 6.05 and 6.02 ppm). First-order rate constants were derived from least-squares best-fit lines of the ln(%) versus time plots. The uncertainty in the reaction rate constants was derived from the slope of the best-fit line. Uncertainties in the activation enthalpy and entropy were calculated from the uncertainties in the slope of the best-fit line of the Eyring plot.

Quantum Chemical Calculations. The geometries of the molecules have been optimized with gradient-corrected density functional theory using the B3LYP²⁶ functional in conjunction with a SVP basis of Ahlrichs et al.²⁷ The nature of the equilibrium structures and transition states was verified by calculating the vibrational frequencies of the optimized species. Improved energies have been obtained at B3LYP using a TZ2P basis set²⁷ at B3LYP/SVP optimized geometries. All calcula-

(26) (a) Becke, A. D. *J. Chem. Phys.* **1993**, *98*, 5648. (b) Lee, C.; Yang, W.; Parr, R. G. *Phys. Rev. B* **1988**, *37*, 785. (c) Stevens, P. J.; Devlin, F. J.; Chablowski, C. F.; Frisch, M. J. *J. Phys. Chem.* **1994**, *98*, 11623.

(27) (a) Schäfer, A.; Horn, H.; Ahlrichs, R. *J. Chem. Phys.* **1992**, *97*, 2571. (b) Schäfer, A.; Huber, C.; Ahlrichs, R. *J. Chem. Phys.* **1994**, *100*, 5829.

(28) (a) Ahlrichs, R. Bär, M.; Häser, M.; Horn, H.; Kölmel, C. *Chem. Phys. Lett.* **1989**, *162*, 165. (b) Treutler, O.; Ahlrichs, R. *J. Chem. Phys.* **1995**, *102*, 346.

tions were carried out with the program package TURBO-MOLE.²⁸

Acknowledgment. This work was supported by the Deutsche Forschungsgemeinschaft (IP 7/5-2; IP 7/5-3). We thank the HRZ Marburg, HLRZ Stuttgart, and the CSC Frankfurt for computer time.

Supporting Information Available: Data of crystal structure determination and refinement, tables of atomic coordinates, interatomic distances and angles, anisotropic thermal parameters, and hydrogen parameters of the compounds **3a** and **4**. This material is available free of charge via the Internet at <http://pubs.acs.org>.

OM0491185